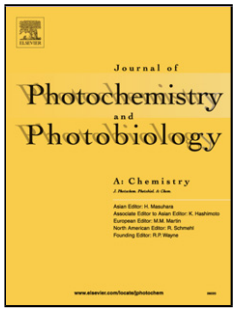

Title: Novel Azobenzene Nickel(II) sensitizer for Dye-Sensitized Solar Cells

Author: Lingyun Zhang Yanan Luo Ruokun Jia Xuhui Sun Chunguang Liu Yingjie Zhang

PII: S1010-6030(15)00427-X
DOI: http://dx.doi.org/doi:10.1016/j.jphotochem.2015.12.001
Reference: JPC 10076

To appear in: *Journal of Photochemistry and Photobiology A: Chemistry*

Received date: 27-5-2015
Revised date: 25-11-2015
Accepted date: 1-12-2015

Please cite this article as: Lingyun Zhang, Yanan Luo, Ruokun Jia, Xuhui Sun, Chunguang Liu, Yingjie Zhang, Novel Azobenzene Nickel(II) sensitizer for Dye-Sensitized Solar Cells, Journal of Photochemistry and Photobiology A: Chemistry http://dx.doi.org/10.1016/j.jphotochem.2015.12.001

Novel Azobenzene Nickel(II) sensitizer for Dye-Sensitized Solar Cells

Lingyun Zhang[a*] zhanglingyun@vip.sina.com, Yanan Luo[b], Ruokun Jia[a], Xuhui Sun[a], Chunguang Liu[a], Yingjie Zhang[a]

[a]School of Chemical Engineering, Northeast Dianli University, Jilin 132012, P. R. China. Fax: +86-432 64806371, Tel.: +86-432 64807273.

[b]College of Chemical and Pharmaceutical Engineering, Jilin Institute of Chemical Technology, Jilin City, Jilin, 132022, P. R. China

[*]Corresponding author.

Graphical Abstract

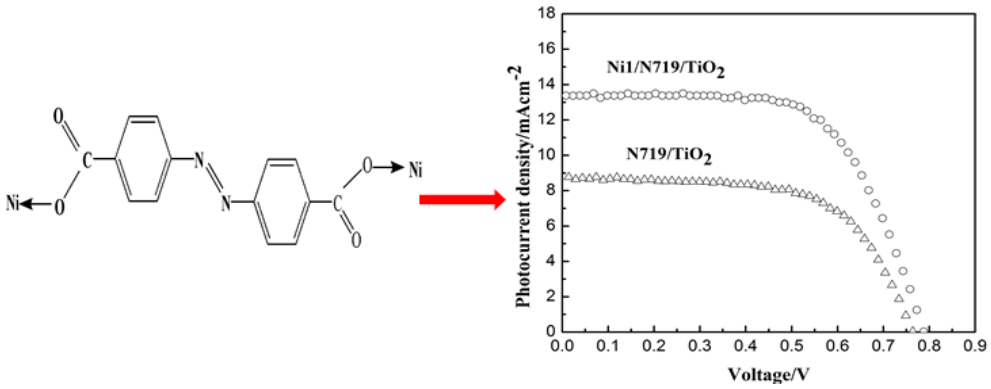

Highlights

- A novel 1-D chain complex was synthesized.
- The complex show photoelectric activity in blue light region.
- The complex was used as a sensitizer for dye-sensitized solar cells.
- The complex improved the efficiency of cells by co-sensitization with N719.

Abstract

A novel 1-D chain complex {[Ni(azobenzene-4,4'-dicarboxylic acid)(ethylenediamine)$_2$](N,N-dimethylformamide)$_2$}(named as **Ni1)** was designed, synthesized, characterized, and demonstrated as an efficient sensitizer for dye-sensitized solar cells. The structure of **Ni1** was characterized by single-crystal X-ray diffraction, infrared (IR) spectra, and elemental analysis. The optical, electrochemical and photovoltaic properties of **Ni1** were investigated by UV-visible spectroscopy, cyclic voltammetry, and the photocurrent-photovoltage measurement. The results show that the incident photo-to-current conversion efficiency of cells based on **Ni1** was obviously improved in blue light region of solar spectra. The overall conversion efficiency of the dye-sensitized solar cells using **Ni1** was increased by 62% under AM 1.5 illumination (100 mW cm^{-2}).

Keywords: Dye-sensitized solar cells; Organic sensitizer; Azobenzene; Co-sensitization; Optical properties

1. Introduction

In the face of the limited fossil fuels and the disastrous environmental problem, people realize the urgent need to develop renewable energy resources for the increasing global energy demand. Solar energy is the most hopeful of supplying sustainable energy because it is a kind of clean and renewable energy. The dye-sensitized solar cells (DSSCs) have attracted much attention as a promising technology for the performance/price ratio cells [1, 2]. The dye is a key component which decides the efficiency of DSSCs as it absorbs sunlight, excites electrons and injects electrons into the conductor band of the semiconductor [3, 4]. In the future, cost-effective organic dyes will play a pivotal role in the large-scale production and application of DSSCs.

To date, the highest conversion efficiency of DSSCs has been achieved by using Ru dyes (N719, N3) [5, 6]. However, Ru dyes have several disadvantages: (1) relatively low extinction coefficients; (2) rare and expensive metal Ru; (3) dye aggregates on the semiconductor; (4) only absorb visible light. Low extinction coefficients make against the improvement of the light harvesting for DSSCs. Using rare metal Ru raises the cost of DSSCs and hampers practical applications of DSSCs. The aggregates of Ru dyes on the semiconductor make against the carrier transport in DSSCs and increase the recombination of excited electrons and injected electrons with I_3^-/I^- in the electrolyte. At present, the main drawback of Ru dyes is the lack of light-absorbing in the blue-violet and red region of solar spectrum. The facts above prompt researchers to develop new-type dyes for the improvement in the efficiency of DSSCs. So far

researchers have synthetized many kinds of dyes. These dyes have high molar extinction coefficients, multiple optical absorption bands in ultraviolet, and visible and near infrared region in spectrum. But the conversion efficiency of these dyes is still behind that of Ru dyes. An approach to the high power efficiency of DSSCs is using the optimal dye that can absorb all sunlight from ultraviolet to near infrared region. Single dye cannot satisfy the demand above. On the basis of these strategies, the combination of mixed dyes is used to solve the previous problem. The light-absorbing response of DSSCs is extended and the aggregates on the semiconductor of dyes are reduced by using two dyes in DSSCs. Although some progresses in the co-sensitization of nanocrystalline TiO_2 with two dyes have been achieved, further investigating the co-sensitization properties of DSSCs with different dyes is still needed. Most co-sensitization systems have supplemented the visible and near infrared spectroscopy, the absorption of blue-violet light is still limited.

In this work, we synthesize a new dye (**Ni1**) using low cost and toxicity metal Ni through a simple method for DSSCs. **Ni1** and N719 are used to co-sensitize TiO_2 film and they present excellent photovoltaic performances. The combination of **Ni1** and N719 has successfully extended the light-absorbing response of DSSCs to the blue region and reduced the aggregates on the semiconductor of dyes.

2. Experimental Section

2.1 Materials and reagents

All chemicals, LiI, I_2, $NiCl_2$, TiO_2, 4-tertbutylpyridine, N,N-dimethylformamide, ethylenediamine, *cis*-bis(isothiocyanato)bis(2,2-bipyridyl-4,4-dicarboxylate]

ruthenium(II) bis-tetrabutylammonium (N719), acetonitrile-propylene carbonate, were analytical grade and were used without further purification. Azobenzene-4,4'-dicarboxylate was synthesized according to a published procedure [7,8].

2.2 Synthesis of Ni1

An aqueous solution (16 mL) containing azobenzene-4,4'-dicarboxylate (5 mg, 0.019 mmol), $NiCl_2$ (30 mg, 0.32 mmol), H_2O (1 mL), DMF (15 mL) and ethylenediamine (0.03 mL) was stirred at room temperature for 30 min until a clear red solution formed, finally transferred into a 25 mL glass bottle and heated to 120 °C for 72 h under autogenous pressure. Afterwards, it was cooled to 25 °C at a rate of 4 °C·h^{-1}. Red sheet crystals were obtained after being washed with DMF and dried in air, in about 38 % yield (based on Ni). Anal. calcd. for $C_{24}H_{38}N_8NiO_6$ (593.33): C 48.54; H 6.60; N 18.84; found: C 48.67; H 6.62; N 18.79. IR data (KBr pellet, cm^{-1}, Figure S1): 3313 (s), 3294 (s), 2943 (w), 1614 (s), 1593 (s), 1535 (s), 1039 (s), 1027 (s), 796 (s), 706 (m), 619 (w), 513 (m).

2.3 Fabrication of DSSCs

A colloidal solution of TiO_2 was obtained by being coated on the fluorine-doped tin oxide (FTO) conducting glass by screen printing and then dried for 6 min at 125 ^oC. The TiO_2 electrodes were gradually heated under an air flow at 325 ^oC for 5 min, at 375 ^oC for 5 min, at 450 ^oC for 15 min, and at 500 ^oC for 15 min. The area of film was 0.25 cm^2. The film electrodes were soaked in the **Ni1** solution (concentration: 5×10^{-4} M, solvent: absolute ethanol for 5 h and N719 solution (concentration: 5×10^{-4} M,

solvent mixture: acetonitrile and absolute ethanol in volume ratio of 1:1) for 20 h at room temperature, respectively. Then, the co-sensitized films were dried in air. The counter electrodes were thermally platinized conducting glass (5 mM H_2PtCl_6 in dry isopropanol, heated at 400 °C for 10 min). The electrolyte was consisted of 0.5 M LiI, 0.05 M I_2, 0.1 M 4-tertbutylpyridine in 1:1 (volume ration) acetonitrile-propylene carbonate.

2.4 Characterization

The elemental analyses were carried out on a Perkin-Elmer 240C elemental analyzer. The IR spectra were recorded (400-4000 cm^{-1} region) on a Nicolet Impact 410 FT-IR spectrometer using KBr pellets. The single-crystal X-ray diffraction data for Ni**1** was collected from a Bruker Apex Ⅱ CCD area-detector diffractometer (Mo *Ka*, 0.71073 Å), operating at 296 ± 2 K. An empirical absorption correction was applied to the date using the SADABS program. The structure was solved by the direct method (SHELXS-97) and refined by full matrix least squares. All non-hydrogen atoms were refined anisotropically. All hydrogen atoms were located geometrically by the program OLEX 2. The final formula was derived from crystallographic data combined with elemental and thermogravimetric analyses data. The CCDC number of Ni**1** is 881780. A summary of the crystallographic data and structural determination for Ni**1** is listed in Table S2. Selected bond lengths and bond angles of Ni**1** are listed in Table S3. Hydrogen bond distances and angles for Ni**1** are listed in Table S4. UV-visible absorption spectra of the samples were measured at room temperature on U-3010 spectrophotometer (Hitachi, Japan) with an integrating sphere (model

130-0632).

2.5 Photoelectrochemical measurements

The photocurrent-photovoltage (*J*-*V*) curves of the sealed cells were measured under AM 1.5 illumination (100 $mW \cdot cm^{-2}$) by using a solar simulator. Electrochemical impedance measurements were carried out by electrochemical work-station (chi660d, Chenhua, China) with three-electrode system in the dark. Frequency range was 0.05-10^5 Hz, and the applied potential was generally between 0～0.700 V. The IPCE spectra were measured with a Model SR830 DSP Lock-In Amplifier and a Model SR540 Optical Chopper (Stanford Research Corporation, USA), a 7IL/PX150 renon lamp as light source, and a 7ISW301 Spectrometer. Cyclic voltammetry experiment was performed with a three-electrode system, a platinum working electrode, a platinum counter electrode, and an Ag/AgCl reference electrode. The potentials were referenced to the ferrocene/ferrocenium (Fc^+/Fc) couple.

3. Results and discussion

The synthetic route of **Ni1** is depicted in Scheme 1. In Ni**1**, L^{2-} ligand adopts μ_2-bidentate mode with the carboxyl group displaying monodentate fashion, as shown in scheme 1. Single-crystal X-ray diffraction analysis reveals that **Ni1** crystallizes in the triclinic system, space group *P*-1, which exhibits an infinite 1D chain structure. As shown in Figure 1, the asymmetrical unit of compound **1** contains one Ni(II) atom, half a L^{2-} ligand, one en molecule and one crystallization DMF molecule. Ni**1** atom is six coordinated by two oxygen atoms from two ligands and four nitrogen atoms from two en molecules, forming a slightly distorted octahedral geometry. The distances of

Ni-O/N [2.076(2) Å-2.132(2) Å] are comparable with those found in other related Ni(II) complexes.

L^{2-} ligands link Ni(II) cations into an infinite 1D chain structure with Ni⋯Ni distance of 17.76 Å, as shown in Figure 2(a). However, it's worth mentioning that the ligands didn't generate any torsion by measuring the dihedral angle between the two benzene rings planes. In the crystal building, each chain interacts with adjacent chains by hydrogen bonds leading to two-dimensional (2D) supramolecular motif. The coordinated en molecules play an important role in the formation of hydrogen bonds. There exist N–H⋯O [N3⋯O2^{iv} = 3.094(4) Å, N3–H3B⋯O2^{iv} = 114°; N4⋯O2^{v} = 3.230(4) Å, N4–H4B⋯O2^{v} = 134°] hydrogen bonds between adjacent chains, linking the 1D chains into a 2D layer structure, as shown in Figure 2(b). In addition, N3 acting as a hydrogen bond donor bonds to O3^{vi} [N3⋯O3^{vi} = 3.163(6) Å, N3−H3A⋯O3^{vi} = 149°) to connect the DMF molecules with 2D layer structure, as shown in Figure 2(c). The hydrogen bond interactions possibly play important roles for constructing and stabilizing the 2D supramolecular structure of Ni**1**.

Figure 3 shows normalized absorption spectra of **Ni1**, mixed dyes of **Ni1** and N719 (1:1 molar ratio) in absolute ethanol solution (10^{-5} mol/L) and mixed dyes of **Ni1** and N719 absorbed on TiO_2 thin film. **Ni1** shows absorbing response in the blue light region (300nm-450nm) with maximum absorption peak at 400nm. The absorption band of **Ni1** is attributed to the π-π* transitions [9,10]. It is well known that absorption band of N719 is in 450 nm-650nm. Therefore, **Ni1** can effectively broaden the absorption response of N719 by the combination of N719 and **Ni1**. The absorption

spectrum of mixed dyes of **Ni1** and N719 in solution exhibits two light absorption band in 300nm-450nm and 450nm-650nm, respectively. As shown in Figure 3, light absorption response is obviously broadened by the combination of **Ni1** and N719. The absorption spectrum of **Ni1** and N719 absorbed on the TiO_2 film exhibits there light absorption bands in 350nm-400nm, 400nm-500nm, and 500nm-650nm, respectively. The absorption bands of **Ni1** (400nm-500nm) has narrowed relative to that in absolute ethanol solution. It is known that the dyes have the strong attractive forces between the molecules at the solid-liquid interface. The attractive forces can lead the shift of absorption peak. The attractive forces have two forms: red-shift J-aggregation and blue-shift H- aggregation. The maximum absorption peak of Ni1 attached to TiO_2 film has obviously red-shifted by 33nm from 400nm to 433nm compared to that in absolute ethanol solution, owing to dye anchoring and J - aggregation on TiO_2 semiconductor surface. The absorption bands of N719 (450nm-650nm) has broadened relative to that in absolute ethanol solution. The maximum absorption peak of N719 has not obviously shift relative to that in ethanol solution. As a whole, the combination of **Ni1** and N719 broadens and intensifies the light absorption of DSSCs, which should be profitable for light harvesting and photocurrent generation in DSSCs.

Figure 4 shows the incident photo-to-current conversion efficiency (IPCE) data of DSSCs based on N719/TiO_2 and **Ni1**/N719/TiO_2 photoelectrodes. The IPCE of DSSCs based on N719/TiO_2 and **Ni1**/N719/TiO_2 photoelectrodes match their absorption spectra, indicating that **Ni1** and N719 anchor on TiO_2 semiconductor surface and possess the ability for photo-induced injection and separation. For

N719/TiO_2 DSSCs, the maximum IPCE value is 59% at about 540nm, which stays in the range of 420nm-670nm. As shown in Figure 4, the IPCE of DSSCs based on **Ni1**/N719/TiO_2 photoelectrode exhibits two peaks, 350nm-450nm with top value of 70% at 400nm and 450nm-700nm with top value of 62% at 520nm, respectively. Compared to that of N719/TiO_2 DSSCs, the combination of **Ni1** and N719 extends the IPCE response to 350nm in the UV light region. In addition, IPCE value in 350nm-530nm increases by the combination of **Ni1** and N719. The co-sensitization of **Ni1** and N719 on TiO_2 film effectively increases the light harvesting of DSSCs, which should improve the conversion efficiency of DSSCs. Moreover, the both ends of IPCE peak for DSSCs based on N719 are low, which is different with the Nazeeruddin's report [11]. Many factors influence the shape of IPCE spectrum, such as the kind of the photoanode, the thickness of the photoanode, the morphology of the photoanode, and composition of the electrolyte [12,13]. The TiO_2 photoanode and composition of the electrolyte in this paper are not the same as that in Nazeeruddin's report. Therefore, the shape of IPCE spectrum shows the difference with that in Nazeeruddin's report. The insufficient driving force for injection of excited N719 molecule and regeneration of the oxidized N719 molecule in our system led to a low electron injection efficiency and light-harvesting efficiency in the UV and red part of the solar spectrum [13].

Cyclic voltammetry is used to study the electrochemical properties of **Ni1**, the mechanism of electron injection from the **Ni1** to conductor band of TiO_2, the oxidation and reduction regeneration of **Ni1** in the electrolyte. Figure 5 shows the cyclic voltammetry of **Ni1** in CH_2Cl_2 solution. **Ni1** exhibits a reversible oxidation-

reduction behavior. The ground-state oxidation potential (E_{ox}) corresponding to the high occupied molecular orbital (HOMO) level is determined by the peak potential of CV [14]. E_{ox} of **Ni1** is 1.71V (vs. NHE), which is more positive than the redox potential of I_3^-/I^- couple (0.4V vs NHE) [15]. It suggests that the oxidized **Ni1** formed after electron injection into the conductor band of TiO_2 should be thermodynamically reduced by I_3^-/I^- in the electrolyte. The absorption threshold of **Ni1** is 450nm, which corresponds to the band gap energy of 2.76 eV according to Eq. (1) [16].

$$E_g(\text{eV})=1240/\lambda(\text{nm}) \qquad (1)$$

The excited-state redox potential (E_{red}) corresponding to the low unoccupied molecular orbital (LUMO) level is calculated to be -1.05V according to Eq. (2) [17].

$$E_{red} = E_{ox} + E_g \qquad (2)$$

E_{red} of **Ni1** is more negative than the bottom of conductor band of TiO_2 (-0.5V vs NHE), which confirms that the electron injection from excited state **Ni1** is thermodynamically favorable. Figure 6 shows the schematic energy levels of **Ni1** based on the absorption and the electrochemical data. The exciting, electron injecting and redox regenerating of **Ni1** are exhibited in Figure 6, indicating **Ni1** can efficiently sensitize TiO_2 photoanode of DSSCs.

Electrochemical impedance spectroscopy (EIS) is used to correlate device structure with a suitable model for the study of kinetics of electron transfer and photoelectrochemical processes which occurred at the interface of DSSCs. Figure 7 shows electrochemical impedance spectroscopy of **Ni1**/N719/TiO_2 and N719/TiO_2-based DSSCs in the dark. In Figure 7a, experimental data are represented

by symbols while the solid lines correspond to the fit obtained by Zsimpwin software using the equivalent circuit $R_s(C_1(R_1O_1))(R_2Q_2)$ [18,19]. The spectra show one large semicircle at medium frequency region and a small semicircle at high frequency region [20,21]. In equivalent circuit, the symbols R and C describe resistance and capacitance, respectively； O, which depends on the parameters $Y_{o,1}$ and B, accounts for a finite-length Warburg diffusion, and Q is the symbol for the constant phase element, CPE (its parameters are $Y_{o,2}$ and n)[20]. $Y_{o,1}$ and $Y_{o,2}$ are Warburg coefficients at the photoanode/dye/electrolyte interface and the Pt/electrolyte interface, respectively, corresponding to the module 1 and 2 in the equivalent circuit. Parameters obtained by fitting the impedance spectra of composite solar cells using the equivalent circuit are listed in table 1. R_s is the series resistance of DSSCs, accounting for the resistance of polymer electrolyte, the resistance within the photoelectrode film and the FTO electrode, as well as contacts. No obvious difference for the series resistance (R_s) is observed between DSSCs based on **Ni1**/N719/TiO_2 (4.09 Ω cm^2) and DSSCs based on N719/TiO_2 (3.43Ω cm^2). R_2 deceases from 16.22 to 8.66 Ω.cm^2 by **Ni1** and N719 co-sensitization. R_2 at high frequency is associated to the resistance at Pt/electrolyte interface. R_2 is the diffusion impedance of I_3^- at the counter electrode. The decrease of R_2 is attributed to the increased activation between I_3^- in the electrolyte and Pt counter electrode. The decrement of diffusion impedance favors the reduction of I_3^- at the counter electrode. When C_1 increase and R_2 decrease, much more I_3^- is reduced at Pt electrode surface [19]. This is propitious to the increase of FF of the DSSCs. C_1 and R_1 at the medium frequency are attributed to the capacitance and charge transfer

resistance of electron transfer process at the TiO_2/dye/electrolyte interface. C_1 increases from 11.96×10^{-4} to 20.31×10^{-4}F.cm^{-2}. The increasing film capacitance means more electrons at the interface of TiO_2/**dye**/electrolyte as the light absorption is enhanced because of **Ni1** and N719 co-sensitization. R_1 slightly deceases from 14.37 to 11.86 Ω.cm^{-2} by **Ni1** and N719 co-sensitization. The decreasing value of R_1 means that the recombination resistance is low at the interface of TiO_2/**Ni1**/N719/electrolyte. The low recombination resistance indicates that the recombination of electrons at the interface of TiO_2/**Ni1**/N719/electrolyte slightly increased. This slight increasing of electron recombination may be caused by the increasing of the injected and excited electrons at the interface of TiO_2/**Ni1**/N719/electrolyte. Meanwhile, the recombination characteristic peak of DSSCs based on **Ni1**/N719/TiO_2 photoanode shifts to a lower frequency (5.52 Hz) compared with that of N719/TiO_2 photoanode (8.16Hz) in Figure 7b. This indicates a longer electron lifetime for DSSCs based on **Ni1**/N719/TiO_2 [22]. The high film capacitance and low recombination characteristic frequency makes the highest η possible [23].

Figure 8 shows the current density versus voltage curves of DSSCs based on the films of **Ni1**/N719/TiO_2 and N719/TiO_2 under 100 mW/cm^2 illumination. The photovoltaic performances of N719/TiO_2-based DSSCs, e.g. the short photocurrent density (J_{sc}), the open circuit voltage (V_{oc}), the fill factor (FF), and overall energy conversion efficiency (η) are 8.78mA/cm^2, 0.76V, 0.62, 4.17%, respectively. Compared with that of N719/TiO_2-based DSSCs, the photovoltaic performances of **Ni1**/N719/TiO_2-based DSSCs have obviously improved as shown in Figure 8. J_{sc} of **Ni1**/N719/TiO_2-based

DSSCs (13.46 mA/cm^2) has a remarkably increase relative to that of N719/TiO_2-based DSSCs (8.78mA/cm^2), meaning much more injection electrons in CB of TiO_2. This increase of J_{sc} indicates that **Ni1** and N719 effectively co-sensitized TiO_2 photoanode and resulted in a higher light harvesting. The V_{oc} increases from 0.76 to 0.79 V by **Ni1** and N719 co-sensitizing. V_{oc} is the difference potential between the electrochemical potential of the redox couple in the electrolyte and the conduction band edge of TiO_2 photoanode [24]. The increase of V_{oc} indicates that co-sensitization of **Ni1** and N719 leads to an upward shift of the conduction band edge of TiO_2 [25]. As shown in table 1, co-sensitization of **Ni1** and N719 decreases the resistance at Pt/electrolyte interface of DSSCs, resulting in the activation or better contact between electrolyte and Pt catalyst. Therefore, FF increases from 0.62 to 0.64. The overall solar conversion efficiency of DSSCs based on **Ni1**/N719/TiO_2 tremendously increases by 62% from 4.17% to 6.77% compared with DSSCs based on N719/TiO_2.

4. Conclusions

In this paper, **Ni1** was designed and synthesized as the dye to sensitize TiO_2 photoanode with N719 for DSSCs application. The combination of **Ni1** and N719 not only extends the photoresponse of DSSCs to the UV region of the solar spectrum but also intensify the optical spectrum absorption. The photovoltaic performances of **Ni1**/N719/TiO_2-based DSSCs obviously improved compared with to DSSCs based on individual dye (N719).

Acknowledgments

This work was supported by the national science foundation of china (grant No. 21373043), Jilin Provincial Science & Technology Department (No.20130305017GX, 20140101090JC, 20130413046GH), scientific research fund of Jilin provincial education department (No.2014105), Jilin city science and technology bureau (201464036), and the Doctor Science Foundation of Northeast Dianli University (No. BSJXM-201321).

References

[1] É. Torres, S. Sequeira, P. Parreira et al, Coumarin dye with ethynyl group as π-spacer unit for dye sensitized solar cells, J. Photoch. Photobio. A. 310:1(2015)1-8.

[2] D. Punnoose, H.J Kim , CH.S.S.P. Kumar, et al, Highly catalytic nickel sulfide counter electrode for dye-sensitized solar cells, J. Photoch. Photobio. A. 306:15(2015)41-46.

[3] P.K. Baviskar, J.B. Zhang, V. Gupta et al, Nanobeads of zinc oxide with rhodamine B dye as a sensitizer for dye sensitized solar cell application, J. Alloy. Compd. 510(2012)33-37.

[4] L. Zhang, Y. Yang, R. Fan et al, The charge-transfer property and the performance of dye-sensitized solar cells of nitrogen doped zinc oxide, Mater. Sci. Eng., **B** (2012)177956-177961.

[5] M. Nazeeruddin, A. Kay, I. Rodicio, Conversion of light to electricity by cis-X_2bis(2,2′-bipyridyl-4,4′-dicarboxylate) ruthenium(Ⅱ) charge-transfer sensitizers (X=Cl^-, Br^-, I^-, CN^-, and SCN^-) on nanocrystalline TiO_2 electrodes, J. Am. Chem. Soc. 115(1993)6382-6390.

[6] P. Wang, Molecular-scale interface engineering of TiO_2 nanocrystals: improving the efficiency and stability of dye-sensitized solar cells, Adv. Mater. 15(2003)2101-2104.

[7] J.S. Park, S. Jeong, S.K. Dho et al, Colorimetric sensing of Cu^{2+} using a cyclodextrinedye rotaxane, Dyes Pigm. 87(2010)49-54.

[8] A. Saylam, Z. Seferoğlu, N. Ertan, Synthesis and spectroscopic properties of new

hetarylazo 8-hydroxyquinolines from some heterocyclic amines, Dyes Pigm. 76(2008)470-476.

[9] S. Gao, R.Q. Fan, L.S. Qiang et al. Effects of solvents and temperature on the luminescence properties of Cd-isonicotinic acid frameworks based on mono-, bi-, and trinuclear cluster units, CrystEngComm. 16(2014)1113-1125.

[10] G.P. Zhou, Y.L. Yang, R.Q. Fan, Syntheses, crystal structures and luminescent properties of three new gallium complexes containing pyridine-2,6-dicarboxylic acid, Chem Res Chinese Universities. 28(2012)936-941.

[11] M. K. Nazeeruddin, S. M. Zakeeruddin, R. Humphry-Baker et al. Acid-Base Equilibria of (2,2'-Bipyridyl-4,4'-dicarboxylic acid)ruthenium(II) Complexes and the Effect of Protonation on Charge-Transfer Sensitization of Nanocrystalline Titania, Inorg. Chem. 38(1999)6298-6305.

[12]G. Calogero, J.H. Yum, A. Sinopoli et al. Anthocyanins and betalains as light-harvesting pigments for dye-sensitized solar cells, Sol. Energy. 86(2012)1563-1575.

[13]Y. Liu, J. R. Jennings, M. Parameswaran et al. An organic redox mediator for dye-sensitized solar cells with near unity quantum efficiency,Energ. & Environ. Sci. 4(2011)564-571.

[14] D. Franchi, M. Calamante, G. Reginato et al, A comparison of carboxypyridine isomers as sensitizers for dye sensitized solar cells: assessment of device efficiency and stability, Tetrahedron. 70(2014)6285-6295.

[15] M. Mao, X.L. Zhang, X.Q. Fang et al, 2,6-conjugated bodipy sensitizers for

high-performance dye-sensitized solar cells, Org. Electron. 15(2014)2079-2090.

[16] M. Guo, P. Diao, Y.J. Ren et al, Photoelectrochemical studies of nanocrystalline TiO_2 co-sensitized by novel cyanine dyes, Sol. Energ. Mat. Sol. C. 88(2005)23-35.

[17] L.Y. Lin, C.H. Tsai, F. Lin et al, 2,1,3-Benzothiadiazole-containing donoreacceptoreacceptor dyes for dye-sensitized solar cells, Tetrahedron. 68(2012)7509-7516.

[18] K.M. Lee, V. Suryanarayan, K.C. Ho, A photo-physical and electrochemical impedance spectroscopy study on the quasi-solid state dye-sensitized solar cells based on poly(vinylidene fluoride-co-hexafluoropropylene, J. Power Sources. 185(2008)1605-1612.

[19] L. Claudia, A.F. Nogueira, M.A. Paoli et al,Solid-state and flexible dye-sensitized TiO_2 solar cells: a study by electrochemical impedance spectroscopy, J. Phys. Chem. B. 106(2002)5925-5930.

[20] Q. Wang, J.E. Moser, M. Grätzel, Electrochemical impedance spectroscopic analysis of dye-sensitized solar cells, J. Phys. Chem. B. 109(2005)14945-14953.

[21] C. He, Z. Zheng, H. Tang et al, Electrochemical impedance spectroscopy characterization of electron transport and recombination in ZnO nanorod dye-sensitized solar cells, J. Phys. Chem. C. 113(2009)10322-10325.

[22] H. Tian, X. Yang, J. Cong et al, Effect of different electron donating groups on the performance of dye-sensitized solar cells, Dyes. Pigm. 84(2010)62-68.

[23] H. Tian, L. Hu, C. Zhang et al, Superior energy band structure and retarded charge recombination for anatase N, B codoped nano-crystalline TiO_2 anodes in

dye-sensitized solar cells, J. Mater. Chem. 22(2012)9123-9130.

[24] L. Zhang, Y. Yang, R.Q. Fan et al, Improvement of efficiency of ZnO-based dye-sensitized solar cells by Pr and N co-doping, J. Mater. Chem. A. 1(2013)12066-12073.

[25] D. Cahen, G. Hodes, M. Gratzel et al, Nature of photovoltaic action in dye-sensitized solar cells, J. Phys. Chem. B. 104(2000)2053-2059.

Figure Captions

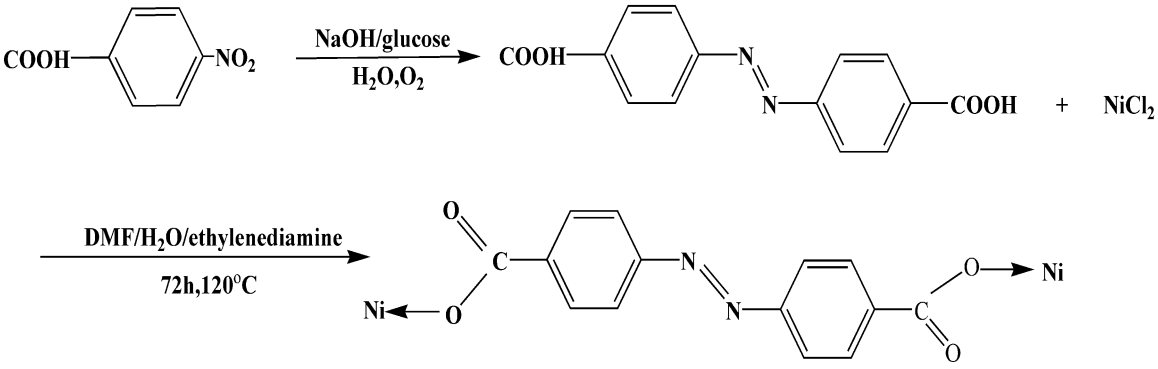

Scheme 1. Synthetic route to **Ni1**

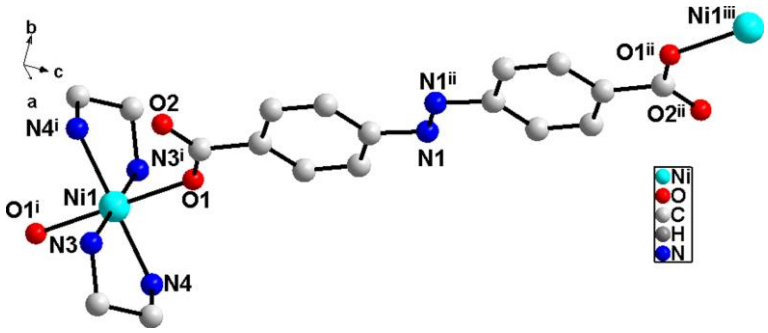

Fig. 1 The coordination environment of **Ni1** (symmetry codes: i, 2-x, -y, -z; ii, 2-x, 1-y, 1-z; iii, x, 1+y, 1+z. All hydrogen atoms are omitted for clarity).

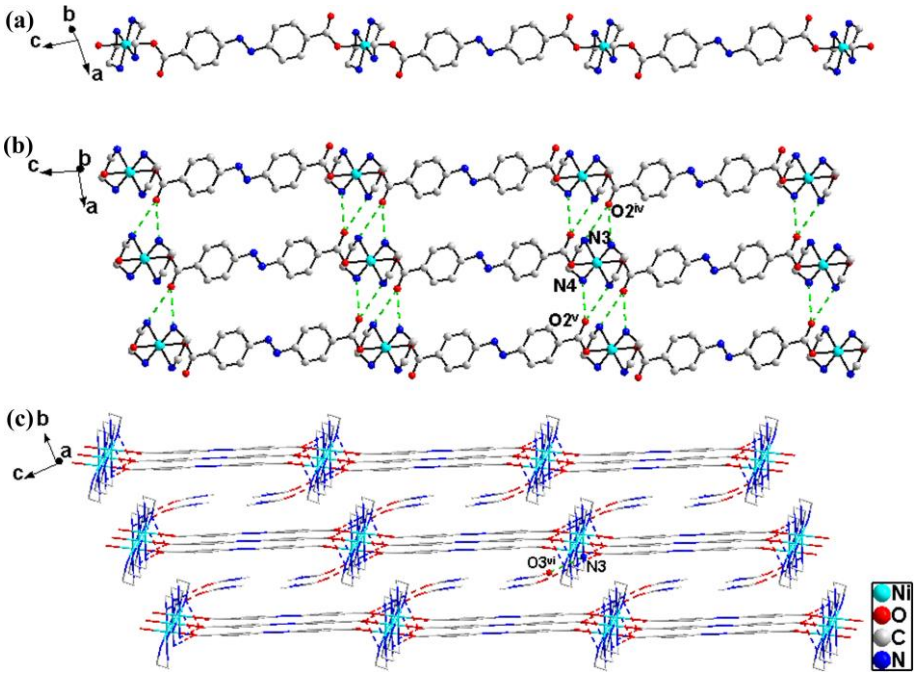

Fig.2 (a) 1D layer constructed from Ni(II) cations and L^{2-} ligands; (b) 1D chain structures are connected into a 2D layer structure; (c) DMF molecules are connected with 2D layer structures *via* hydrogen bond interactions in **Ni1** (symmetry codes: iv, 1-x, -y, -z; v, 1+x, y, z; vi, x, –1+y, z. All hydrogen atoms are omitted for clarity).

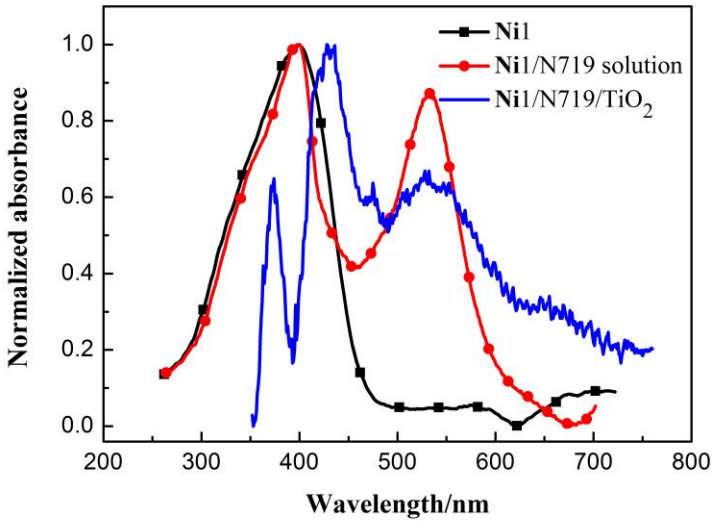

Fig. 3 Normalized absorption spectra of **Ni1**, mixed dyes of **Ni1** and N719 in absolute ethanol solution and mixed dyes of **Ni1** and N719 absorbed on TiO_2 thin film

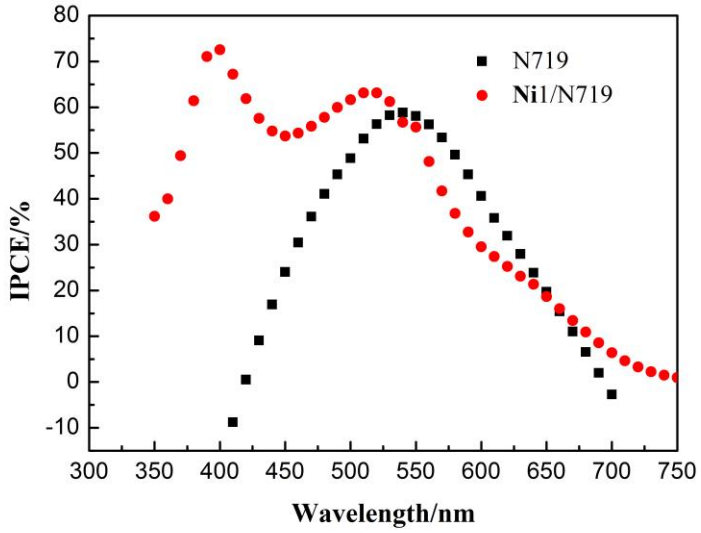

Fig. 4 IPCE spectra of DSSCs based on N719/TiO_2 and **Ni1**/N719/TiO_2 photoelectrodes

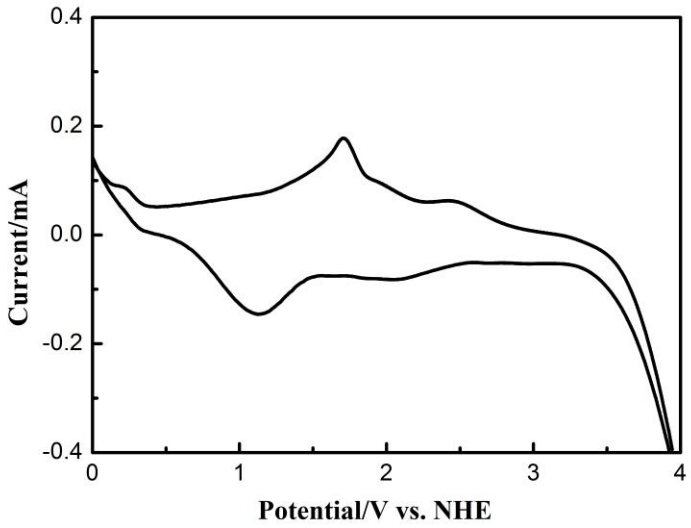

Fig. 5 Cyclic voltammogram of **Ni1** in CH_2Cl_2 solution at scan rate of 100 mV S^{-1}

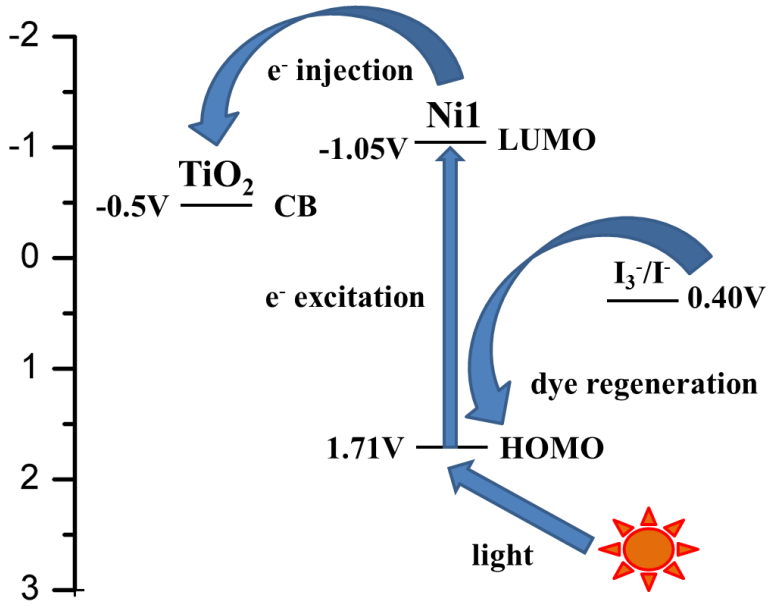

Fig. 6 LUMO and HOMO energy levels of **Ni1** with respect to the conductor band (CB) edge and the valence band (VB) edge energies of TiO_2 and the I_3^-/I^- redox potential.

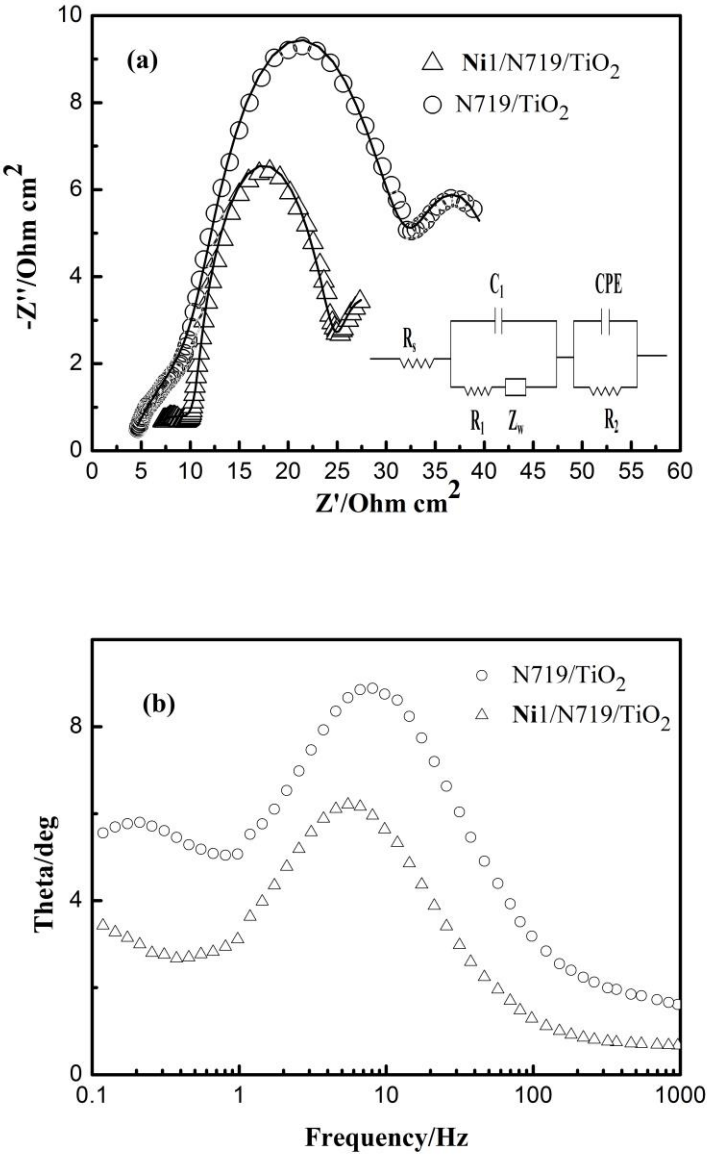

Fig. 7 (a) EIS spectra of DSSCs based on **Ni1**/N719/TiO_2 and N719/TiO_2 in the dark.

(b) Bode phase plots of DSSCs

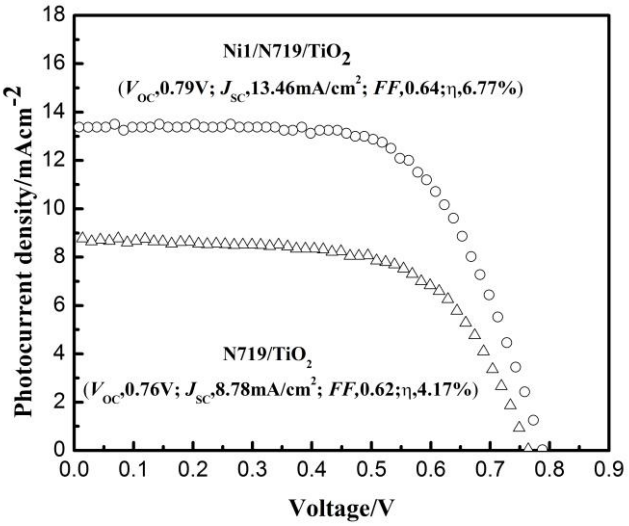

Fig. 8 The current density versus voltage curves of DSSCs based on **Ni1**/N719/TiO_2 and N719/TiO_2 under 100 mW/cm^2 illumination.

Tables

Table 1 Parameters obtained by fitting the impedance spectra of composite solar cells using the equivalent circuit.

DSSC samples	R_s/Ω	C_1/F cm^{-2}	R_1/Ω cm^2	$Y_{O,1}$/S$^{1/2}$ cm^{-2}	B/ΩS$^{1/2}$	R_2/Ω cm^2	$Y_{O,2}$/S$^{1/2}$	n
N719/TiO$_2$	3.43	11.96E-4	14.37	14.51 E-2	1.49	16.22	10.77E-3	0.8
Ni1/N719/TiO$_2$	4.09	20.31E-4	11.86	28.72 E-2	2.04	8.66	10.11E-3	0.8